Am J Cancer Res 2023;13(7):2906-2921
www.ajcr.us /ISSN:2156-6976/ajcr0149660

Original Article

Circular RNA circTIE1 drives proliferation, migration, and invasion of glioma cells through regulating miR-1286/TEAD1 axis

Fubin Li[1*], Lin Wu[2*], Bin Liu[3], Xiangyang An[1], Xinrui Du[1]

[1]Department of Neurosurgery, Zibo Central Hospital, Zibo 255036, Shandong, China; [2]Department of Pediatrics, Zhangdian Maternal and Child Health Care Hospital, Zibo 255036, Shandong, China; [3]Department of Neurosurgery, The First Affiliated Hospital of Shandong First Medical University & Shandong Provincial Qianfoshan Hospital, Jinan 250014, Shandong, China. [*]Equal contributors.

Received February 14, 2023; Accepted June 11, 2023; Epub July 15, 2023; Published July 30, 2023

Abstract: Recent studies have verified that circRNAs (circular RNAs) play a critical role in glioma occurrence and malignant progression. However, numerous circRNAs with unknown functions remain to be explored with further research. qPCR (quantitative real-time polymerase chain reaction) was employed to detect circTIE1 expression in glioma tissues, NHAs (normal human astrocytes), and glioma cellular lines (U87, U118, U251, T98G, LN229). Cell viability was evaluated by CCK-8 assay. Cellular proliferation was evaluated by a 5-ethynyl-2'-deoxyuridine (EdU) proliferation assay. Cell migration and aggression were both evaluated by transwell and migration assays. The direct binding and regulation among circTIE1, miR-1286 and TEAD1 was identified by western blotting, qPCR, luciferase reporter assay, and RNA immunoprecipitation (RIP) assay. Xenografts were generated by injecting glioma cells orthotopically into the brains of nude mice. Immunohistochemistry staining was implemented to evaluate the expression of the proliferation markers ki67 and TEAD1. We found that circTIE1 (circBase ID: hsa_circ_0012012) was upregulated in glioma tissues and glioma cellular lines in contrast to NBT (normal brain tissues) and NHA. CircTIE1 knockdown inhibited glioma cell viability, proliferation, migration and aggression both in vitro and in vivo. Mechanistically, circTIE1 could upregulate TEAD1 expression via miR-1286 sponging, and TEAD1 is a well-known functional gene that could promote malignant advancement in glioma. This research found a novel circRNA, circTIE1, which is an essential marker of glioma progression and diagnosis and may be anticipated to become a crucial target for molecular targeted therapy of glioma.

Keywords: Glioma, circTIE1, miR-1286, TEAD1, proliferation

Introduction

Glioma is the most common primary malignant neoplasm of the brain among adults and has a high disability rate, high mortality and a high recurrence rate [1]. Its incidence rate ranges from 4/100000 to 10/100000 every year. The 5-year mortality rate is second only to pancreatic and lung cancer in general, which has caused a heavy burden on patients, their families, and society [2]. Although the treatment of glioma advocates a multidisciplinary team (MDT) and individual comprehensive treatment with surgery, radiotherapy, chemotherapy, and other therapies, the survival time of patients is still not ideal [3]. Especially for sick persons suffering from glioblastoma, the median survival time is lower than 14.6 months [4]. Recently, with deep studies about the molecular system of comprehending the occurrence and advancement of glioma, searching for glioma-related genes can not only be used to assist in the diagnosis and prognosis evaluation of glioma but also put forward the view of molecular targeted therapy, which has become one of the most promising new therapeutic schemes to cure malignant tumors [5].

CircRNAs are a category of covalently closed single-stranded RNAs that widely exist in nature [6]. Many studies have shown that circRNAs take the lead in carcinoma development and could be considered to be possible carcinoma biomarkers and therapeutic targets [7]. In glio-

ma, several circRNAs associated with the occurrence and advancement of malignant neoplasms have been found [8]. For example, circKIF4A is upregulated in glioma and promotes the growth of glioma and temozolomide resistance by accelerating glycolysis [9]. Circ_0001367 is downregulated in glioma tissues and impedes glioma proliferation, migration and invasion via miR-431-regulated NRXN3 [10]. However, compared with the large number of circRNAs, there are still a large number of circRNAs with unknown functions to be further studied and excavated [11].

The competing endogenous RNA (ceRNA) hypothesis provides a regulatory mechanism for RNA interaction [12]. MicroRNAs (miRNAs) can cause the silencing of functional mRNA by immediately binding to the mRNA sequence 3'-UTR [13]. Conversely, the RNA molecules with identical miRNA binding sites could compete to tie to the miRNAs so that the two RNA molecules can adjust by means of the miRNA bridge. CeRNA molecules encompass circRNAs, lncRNAs, mRNAs, and pseudogenes [14]. As circRNAs are usually produced by unique variable splicing, more than 80% of circRNAs contain exons encoding proteins, which have identical sequences with homologous mRNA and can act as ceRNAs with each other via miRNA sponging [15]. For example, circCHAF1A was upregulated inside glioma and elevated tumorigenesis and proliferation of glioma by means of miR-211-5p-mediated HOXC8 [16].

In our research, we discerned an emerging circRNA by means of circRNA sequencing. CircTIE1 (circBase ID: hsa_circ_0012012) was obviously adjusted inside the glioma in contrast to NBT. Functionally, circTIE1 knockdown obviously inhibited glioma cell viability, proliferation, migration, and aggression both in vitro and in vivo. Mechanistically, circTIE1 could upregulate TEAD1 via miR-1286 sponging. TEAD1 is a known functional gene that can promote the malignant progression of glioma. Our study confirmed that circTIE1 is an essential marker of glioma progression and diagnosis and might be anticipated to become a critical target for molecular targeted therapy of glioma.

Materials and methods

Clinical specimens

This research was endorsed by the Ethics Committee of Zibo Central Hospital. Synchronously, all subjects signed an informed consent form prior to surgery. A total of 35 glioma samples were collected between January 2019 and November 2022. Among them are ten cases with WHO grade II, fifteen with WHO grade IV and ten with WHO grade III. Moreover, another 10 glioma samples obtained through the adjoining NBT were also collected to compare glioma and NBT.

Cell treatment

The glioma cell system (U87, U251, and T98G) originated in the Cell Center of the Chinese Academy of Sciences (Shanghai, China). The normal human astrocytes and glioma cell system U118 were purchased from iCell Bioscience (Shanghai, PR China). LN229, the glioma cell line, was purchased from the American Type Culture Collection (ATCC, Manassas, VA, USA). The whole glioma cell system was fostered in Dulbecco's Modified Eagle's Medium (DMEM, HyClone, Logan, UT, USA), supplemented with 10% fetal bovine serum (FBS; Gibco, Carlsbad, CA, USA) and 1% streptomycin/penicillin (Gibco) with 5% CO_2 at 37°C.

Transfection

The circTIE1 and TEAD1 overexpression plasmids (GenePharma Co., Ltd., Shanghai, China) were constructed using a pLVX vector. Two small interfering RNAs (siRNAs, GenePharma) against circTIE1 were used to silence circTIE1 expression. CircTIE1-KD1: F: 5'-GTGAGAAGCAGGGCGAGGA-3'; R: 5'-UCUCCUCGCCCUGCUUCUC-3'; CircTIE1-KD2: F: 5'-TGAGTGAGAAGCAGGGCGA-3'; R: 5'-UCGCCCUGCUUCUCACUCA-3'; CircTIE1-NC: F: 5'-AACAGUCGCGUUUGCGACU-3'; R: 5'-CCAGUCGCAAACGCGACUG-3'. The mimic, inhibitor and negative control of miR-1286 all originated in Thermo Fisher Scientific (Assay ID: MH13649 and MC13649; Thermo Fisher Scientific, Waltham, MA, USA). All transfected glioma cells were cured by means of puromycin (Sigma, Santa Clara, CA, USA) at a 10 μg/ml concentration for fifteen days. Furthermore, the transfection effectiveness was verified by western blotting or qPCR.

Quantitative real-time polymerase chain reaction (qPCR)

TRIzol reagent (Invitrogen, Carlsbad, CA, USA) was utilized to absorb the glioma cells' whole RNAs. We also used a TaqMan reverse transcription kit (Thermo Fisher Scientific) to per-

form reverse transcription to generate complementary DNA (cDNA). Then, the cDNAs were treated with Power SYBR Green Master Mix (Applied Biosystems, Foster City, CA, USA) or TaqMan MicroRNA Assays (Thermo Fisher Scientific, Inc.) to perform the qPCR assays. The corresponding RNA expression was determined using the 2-ΔΔCt method. Furthermore, β-actin was used as an internal reference. The primer sequences were as follows: circTIE1, F: 5'-TGGGACAGCCTCTACCCTTAG-3' and R: 5'-GTCAAGGTCCCTGAGCTGAA-3'; TEAD1, F: 5'-ATGGAAAGGATGAGTGACTCTGC-3' and R: 5'-TCCCACATGGTGGATAGATAGC-3'; β-actin, F: 5'-TGGGACAGCCTCTACCCTTAG-3' and R: 5'-GTCAAGGTCCCTGAGCTGAA-3'.

RNase R assay

The total RNA extracted from glioma cells was cured by RNase R enzyme (Geneseed, Guangzhou, China) at a concentration of 20 U/μL and fostered at 37°C for thirty min. Next, the whole RNA was explored with qPCR.

Western blotting

All protein from glioma cells was collected via protein lysis buffer (Beyotime Biotechnology, Beijing, China). Moreover, protein samples with equivalent amounts (μg) were subjected to 10% dodecyl sulfate-polyacrylamide gel electrophoresis. Then, the gels were delivered to one nitrocellulose membrane. Moreover, the membrane was blocked by means of 2% bovine serum albumin (Beyotime Biotechnology). Afterward, those membranes were cultivated by anti-TEAD1 or anti-β-actin (Abcam, Shanghai, China) at 4°C during the night and fostered by the secondary antibody (Abcam) the next day. Finally, the protein bands were viewed by employing an improved chemiluminescence (ECL) detection kit (Beyotime Biotechnology), and the band densities were quantified by ImageJ software (National Institutes of Health, Bethesda, MD, USA).

Cell counting kit-8 (CCK-8) assay

Glioma cells during the exponential growth stage were inoculated in 96-well plates at a density of 1×10^3 cells/100 μL/well, with four replicate wells per group. Next, the cells were incubated with 10 μL of CCK-8 solution (Beyotime Biotechnology) for two hours for 1, 2, 3, 4 and 5 days. Each well's A (absorbance) value at 450 nm was gauged by means of one microplate reader.

5-ethynyl-2'-deoxyuridine (Edu) proliferation assay

Glioma cells in the exponential growth phase were inoculated in 24-well plates at a density of 1×10^5 cells per well for twenty-four hours. Next, the cells were treated with EdU reagent (Beyotime Biotechnology) for 2 hours at 37°C. Finally, the cells were fixed with paraformaldehyde. Simultaneously, DAPI (Sigma) was adopted to stain the nuclei. Edu-positive cells were viewed by means of one laser scanning confocal microscope (Olympus, Tokyo, Japan).

Transwell assay and migration assay

For the transwell assay, the upper transwell system chamber (8 μm) was coated with 100 μl of Matrigel (BD Biosciences, CA, USA) for 30 min at 37°C. Then, glioma cells in the exponential growth phase were inoculated in the upper chamber and treated with DMEM supplemented with 0.2% FBS, while the lower chamber was treated with DMEM supplemented with 20% FBS. After 20 h of incubation, the cells in the lower chamber were fixed with 4% paraformaldehyde and stained with H&E (hematoxylin and eosin). The invasive numbers of glioma cells were counted under an inverted microscope (Olympus). In view of the migration assay, glioma cells were directly inoculated into the upper chamber without coating with Matrigel, and the following steps were similar to the transwell assay.

Luciferase activity analysis

Forecast of binding sites between circTIE1 and miR-1286 was obtained from the circInteractome database (https://circinteractome.nia.nih.gov). Forecasts of the binding sites between TEAD1 and miR-1286 were obtained from the starBase database (https://starbase.sysu.edu.cn). Next, wild-type circTIE1, wild-type TEAD1, mutant-type circTIE1, and mutant-type TEAD1 were designed, cloned into the empty pmiRGLO luciferase reporter vector (Promega) and transfected into glioma cells. Finally, a luciferase reporter assay system (Promega) was employed to test the luciferase activity.

RNA immunoprecipitation (RIP) assay

The interaction between circTIE1 and miR-1286 was carried out via a Magna RIP RNA Binding Protein Immunoprecipitation Kit (Millipore, Darmstadt, Germany) according to the manufacturer's guidelines. Glioma cells were lysed with RIP lysis buffer and treated with magnetic beads combined with antibodies against IgG or Ago2 as a passive control. Then, the RNAs binding with Ago2 were immunoprecipitated and incubated with qPCR, and proteinase K was employed with the aim of exploring the enrichment of miR-1286 and circTIE1.

Xenograft experiments

Glioma cells in the exponential growth stage were orthotopically injected into the brains of 6-week-old female BALB/c nude rats (Shanghai SLAC Laboratory Animal Co., Ltd., Shanghai, China) at a density of 1×10^4 cells per mouse. Then, the mice were observed every day for death or neurological symptoms, including hunched back, loss of body weight, reduced food consumption, and inactivity [17]. Moreover, the tumor dimension was gauged as $V = (D \times d^2)/2$. D means the longest diameter; d indicates the shortest neoplasm diameter. The log-rank trial and Kaplan-Meier dissection were employed with the aim of analyzing the survival rates between each group. All animal tests were carried out following the guidelines of the Animal Care Committee of Zibo Central Hospital.

Immunohistochemistry (IHC)

The mouse xenograft tumor specimens were placed in paraffin before being split into 4 μm parts. Next, the paraffin-embedded sections were rehydrated, dewaxed, and antigen-retrieved, and endogenous peroxidases were blocked using immunohistochemistry (Beyotime Biotechnology). The primary antibody against ki-67 or TEAD1 (1:100, Abcam) was applied, and the DAB Substrate Kit (Abcam) was adopted for staining. Stained sections were imaged with a light microscope (Olympus), and the immunohistochemical results were assessed in light of the German immunohistochemical score [18].

Bioinformatic analyses

The prediction of candidate miRNAs for circTIE1 was obtained from the circInterome database (https://circinteractome.nia.nih.gov) and Cancer-Specific CircRNA Database 2.0 (CSCD, http://geneyun.net/CSCD2/#). The prediction of candidate mRNAs for miR-1286 was obtained from TargetScan (http://www.targetscan.org/vert_71/), MiRDB (http://mirdb.org), miRPathDb 2.0 (https://mpd.bioinf.uni-sb.de/overview.html), miRWalk (http://mirwalk.umm.uni-heidelberg.de), and starBase (starbase.sysu.edu.cn).

Statistical analysis

The statistical analysis and related data were implemented by means of GraphPad Prism 8.0 (GraphPad Software Inc., San Diego, CA, USA). All tests were repeated more than 3 times. At the same time, the results are depicted as the mean ± standard error. The chi-square test, t test or F test were utilized with the intention of comparing each group. Statistical significance was stated as a P value < 0.05.

Results

CircTIE1 is upregulated in glioma tissues and cell lines

To explore the possible function of circRNAs in glioma, we carried out circRNA sequencing and discovered that circTIE1 (circBase ID: hsa_circ_0012012) was one of the most significantly upregulated circRNAs in glioma (**Figure 1A-C**). Compared with normal brain tissue (NBT), the logFC value of circTIE1 expression in glioma tissues was 2.871 ($P < 0.001$) (**Figure 1A-C**). The mode diagram of circTIE1 is shown in **Figure 1D**. It can be seen that circTIE1 is composed of the 17-19th exon of the TIE1 transcript via reverse splicing. Sanger sequencing confirmed that the head-tail junction site was G-C (**Figure 1E**). Since circRNAs can tolerate RNase R digestion, we conducted an RNase R assay and found that after RNase R treatment, the TIE1 mRNA level was apparently reduced, while the circTIE1 level was not obviously reduced, confirming that circTIE1 has a circular structure (**Figure 1F**, **1G**). Since the distribution of circRNA in cells has an essential impact on its function, we conducted a FISH assay and found that circTIE1 is largely in the cytoplasm of LN229 and T98G glioma cells (**Figure 1H**). To verify the expression of glioma circTIE1, we explored circTIE1 expression among ten glioma tissues and their adjoining NBTs by means of qPCR and discovered that the expression in glioma tissues evidently exceeded that in adjacent NBTs (**Figure 1I**). Furthermore, qPCR was

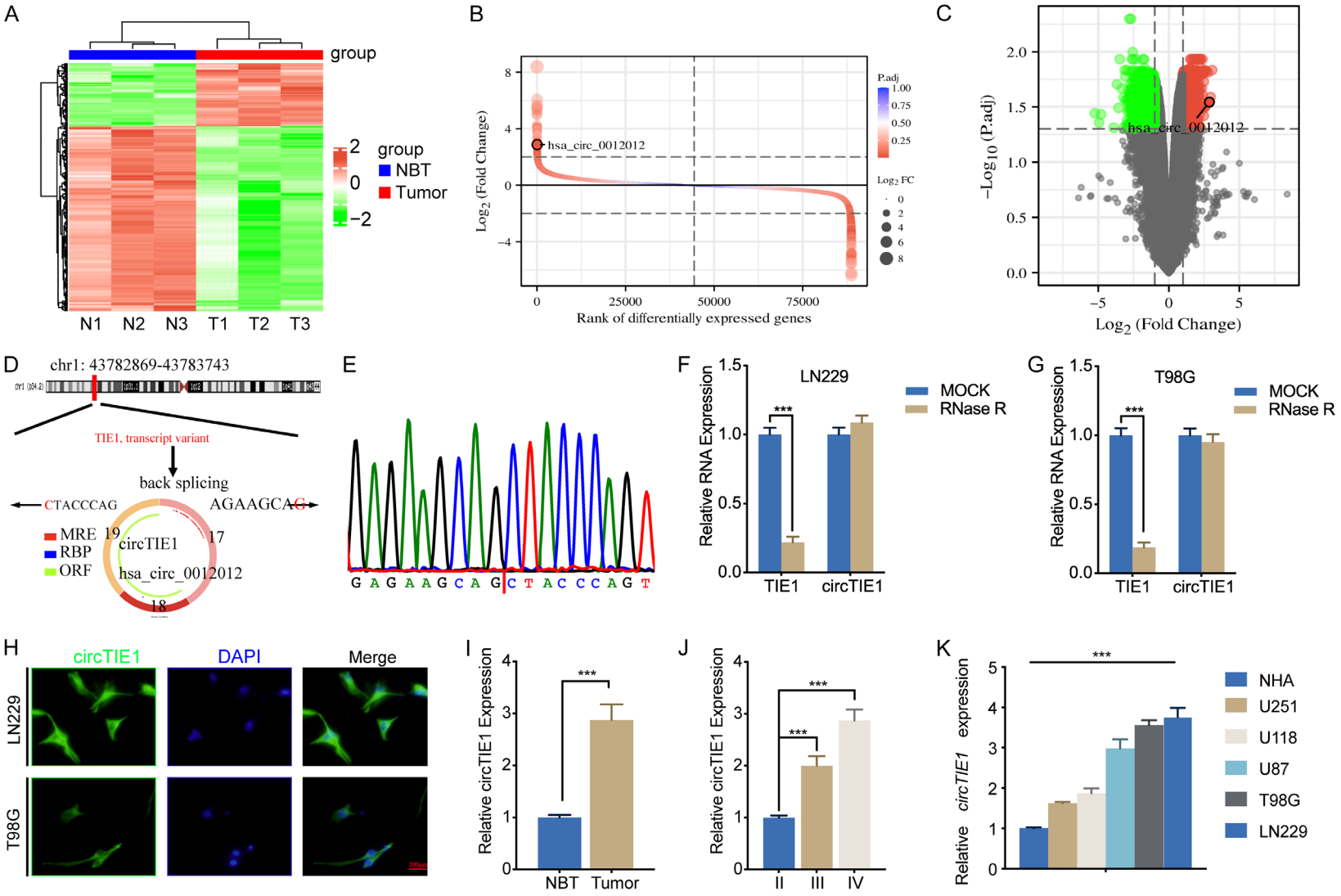

Figure 1. CircTIE1 is up-regulated in glioma tissues and cell lines. (A-C) CircRNA sequencing found the up-regulated circTIE1 expression in glioma tissues. The results were shown by heatmap (A), difference ranking plot (B) and a volcano plot (C). (D) The structure pattern diagram of circTIE1. (E) Sanger sequencing validated the head-tail junction site of circTIE1. (F, G) The effect of RNase R treatment on the expression of TIE1 mRNA and circTIE1 according to qPCR. (H) FISH assays detected the distribution of circTIE1 in glioma cell lines LN229 and T98G. (I) qPCR showed the circTIE1 expression between glioma tissues and adjacent normal brain tissues. n = 10. (J) qPCR showed the circTIE1 expression in glioma tissues with different WHO grades (WHO II, n = 10, III, n = 10, IV, n = 15). (K) qPCR showed the circTIE1 expression in normal human astrocytes (NHA) and glioma cell lines (U87, U118, U251, T98G, LN229). All data are shown as the mean ± SD (three independent experiments). **P < 0.05; **P < 0.01; ***P < 0.001.*

performed on 35 glioma tissues of disparate WHO grades. In addition, it was found that the expression of circTIE1 was upregulated with increasing WHO grade, and its expression was highest in grade IV (**Figure 1J**). In addition, we detected circTIE1 expression in normal human astrocytes and glioma cells and discovered that circTIE1 expression in glioma cell lines significantly surpassed that in normal human astrocytes, and the highest expression was found in T98G and LN229 cells (**Figure 1K**). The results above show that circTIE1 is highly expressed in glioma cells and tissues.

CircTIE1 knockdown inhibits the proliferation and invasion of glioma cells

Since circTIE1 was upregulated inside glioma, its possible biological function in glioma was deeply explored. First, we selected the glioma cell lines LN229 and T98G with the highest circTIE1 expression to knock down circTIE1. qPCR confirmed that the transfection effect of circTIE1 knockdown was stable and reliable (**Figure 2A**). Subsequently, MTS assays were used to detect glioma cell viability. The absorbance values of LN229 and T98G cells decreased significantly after circTIE1 knockdown, which confirmed that circTIE1 knockdown could inhibit glioma cell viability (**Figure 2B**, **2C**). Second, we conducted EdU assays and found that the EdU-positive rates of T98G and LN229 cells were obviously reduced after the knockdown of circTIE1, which confirmed that cell proliferation activity decreased significantly (**Figure 2D**). In addition, we conducted transwell and migration assays and found that the invasion and migration abilities of LN229 and T98G cells were obviously reduced after circTIE1 knockdown, which confirmed that their invasion and migration abilities were significantly reduced (**Figure 2E**, **2F**).

CircTIE1 targets miR-1286 in glioma cells

Since FISH assays confirmed that circTIE1 is chiefly in the glioma cytoplasm, we speculate that circTIE1 may play a part in promoting the malignant advancement of glioma through competing endogenous RNAs (ceRNAs) [19]. We first used the circIntercome and CSCD databases to predict the possible target miRNAs of circTIE1 and found six intersecting miRNAs (**Figure 3A**). To determine the precisely targeted miRNA, both miRNA mimics and inhibitors were used to treat LN229 and T98G cells, respectively, and we found that only miR-1286 can regulate circTIE1 (**Figure 3B-E**). The results indicated that after miR-1286 simulation therapy, the expression level of circTIE1 was significantly decreased (**Figure 3B**, **3C**), while after miR-1286 inhibitor treatment, the circTIE1 expression level was obviously increased (**Figure 3D**, **3E**). We also detected the expression of miR-1286 after circTIE1 knockdown. The results indicated that miR-1286 expression was upregulated (**Figure 3F**). Simultaneously, we analyzed the specific target site between circTIE1 and miR-1286 via the circIntercome dataset. We designed luciferase reporter assays (**Figure 3G**). The circTIE1 wild-type group was treated with the miR-1286 mimic, and its luciferase reporter activity was significantly reduced. In contrast, the circTIE1 mutant group showed no significant change (**Figure 3H**, **3I**). In addition, as AGO2 is the nuclear part of the RISC (RNA-induced silencing complex) connecting miRNAs to their mRNA or miRNA targets, immunopurification of AGO2 can result in binding between miR1286 and circTIE1 [20]. We further performed anti-AGO RIP assays and found that the enrichment of circTIE1 and miR-1286 levels in the AGO treatment group was obviously higher than that in the IgG group. After miR-1286 mimic treatment, miR-1286 and circTIE1 level enrichment in the anti-AGO group further increased (**Figure 3J-M**). The above experimental results show that circTIE1 can bind to miR-1286 and play a regulatory role.

MiR-1286 inhibitor reverses the inhibitory effects of circTIE1 knockdown in glioma cells

In view of the fact that circTIE1 can target miR-1286, we further explored whether the mechanism of circTIE1 promotes glioma cellular proliferation and aggression by means of miR-1286. We implemented rescue tests and administered miR-1286 inhibitor treatment to circTIE1 knockdown glioma cell lines. EdU and MTS assays indicated that cellular viability and proliferation were significantly reduced after circTIE1 knockdown, while cell viability and proliferation were significantly restored after miR-1286 inhibitor treatment (**Figure 4A-C**). Transwell and migration assays also showed that the quantity of cellular migration and aggression were significantly reduced after circTIE1 knockdown, while the quantity of cellular migration and aggression were effectively restored after treatment with the miR-1286 inhibitor (**Figure**

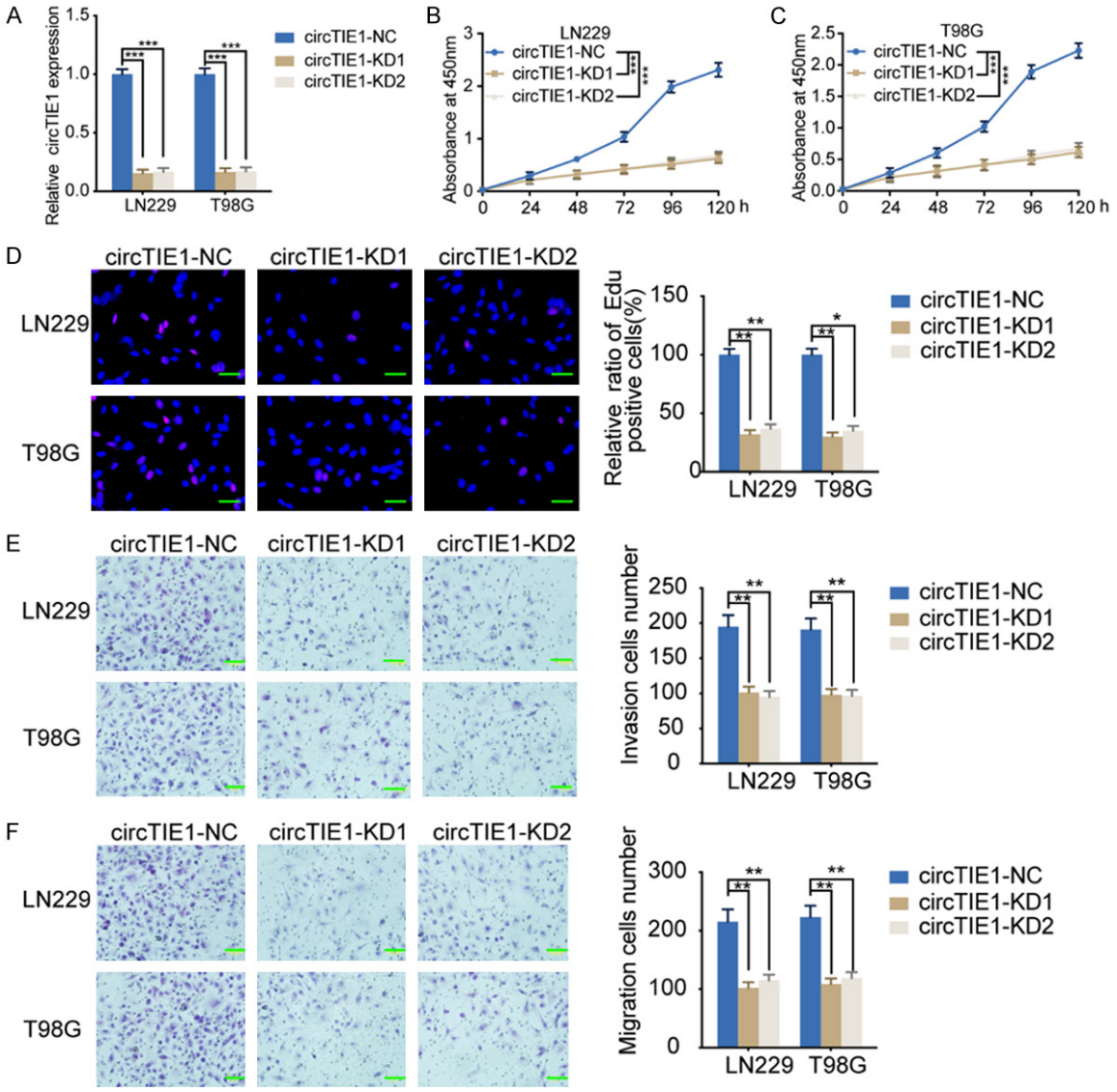

Figure 2. CircTIE1 knockdown inhibits the proliferation and invasion of glioma cells. A: qPCR showed the expression of circTIE1 in LN229 and T98G after transfected siRNA-mediated circTIE1 knockdown. B, C: MTS assays showed the cell viability of glioma cell lines LN229 and T98G after circTIE1 knockdown. D: Representative images of Edu assays showed the proliferation of glioma cell lines LN229 and T98G after circTIE1 knockdown. Scale bar = 50 μm. E: Representative images of transwell assays showed the invasion capacity of glioma cell lines LN229 and T98G after circTIE1 knockdown. Scale bar = 50 μm. F: Representative images of migration assays showed the migration capacity of glioma cell lines LN229 and T98G after circTIE1 knockdown. Scale bar = 50 μm. All data are shown as the mean ± SD (three independent experiments). **P < 0.05; **P < 0.01; ***P < 0.001.*

4D, **4E**). The results above confirmed that circTIE1 promotes the aggression and proliferation of glioma cells through miR-1286.

MiR-1286 directly targets TEAD1 in glioma cells

To deeply investigate the exact mechanism by which miR-1286 promotes glioma cells, we used TargetScan, miRDB, miRWalk, miRPathDB and starBase to forecast the targeted downstream miR-1286 genes and discovered two target genes, namely, PISD and TEAD1 (**Figure 5A**). To determine the exact gene, glioma cells were treated with miR-1286 simulation and inhibitor. Western blotting and qPCR indicated that only the TEAD1 expression level had consistent changes. After miR-1286 mimic treatment, TEAD1 expression decreased significantly, while TEAD1 expression increased significantly after miR-1286 inhibitor treatment (**Figure 5B-G**). However, the PISD expression

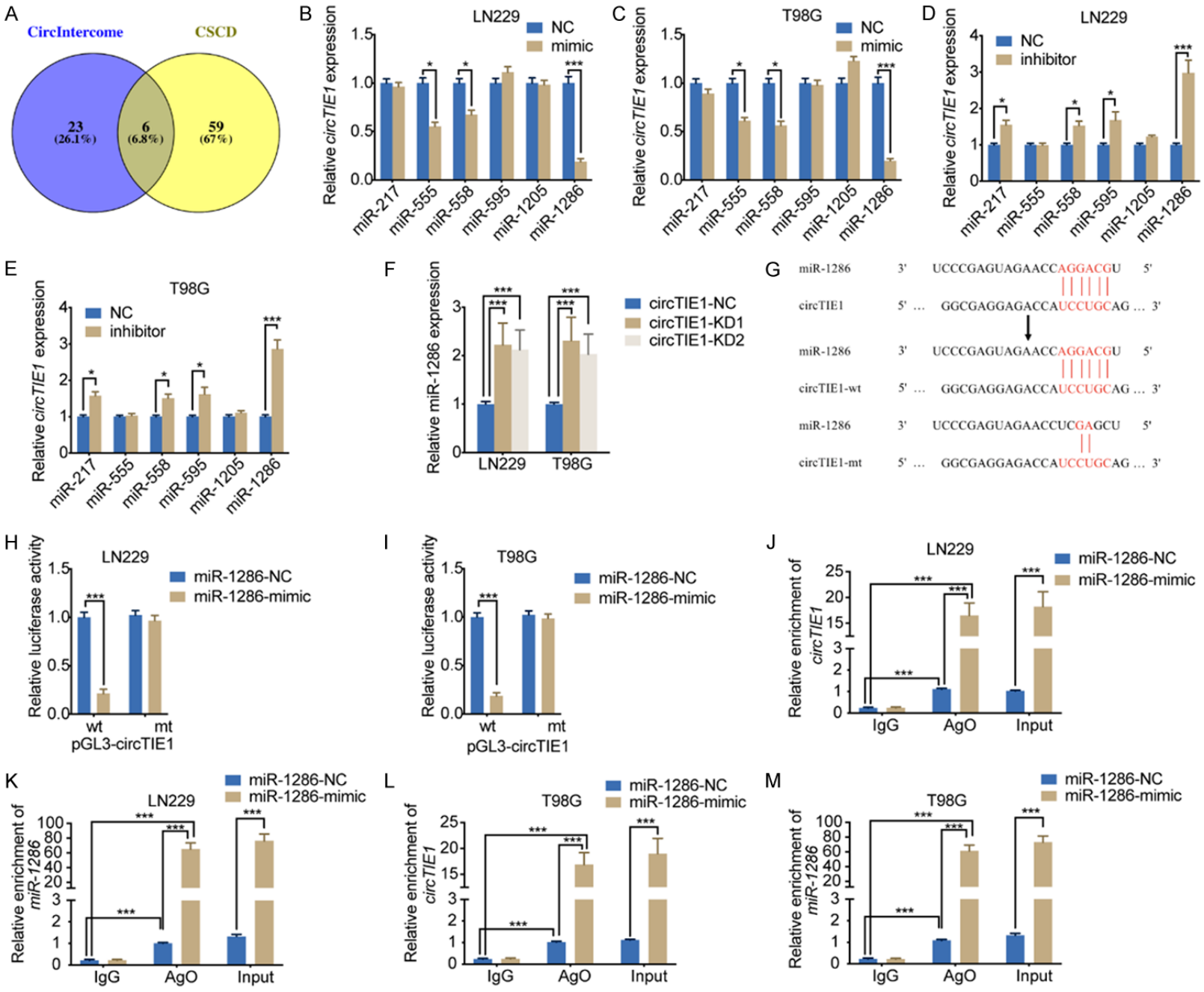
A
CircIntercome
CSCD
23
(26.1%)
6
(6.8%)
59
(67%)
B
LN229
NC
mimic
Relative circTIE1 expression
miR-217
miR-555
miR-558
miR-595
miR-1205
miR-1286
C
T98G
NC
mimic
Relative circTIE1 expression
D
LN229
NC
inhibitor
Relative circTIE1 expression
E
T98G
NC
inhibitor
Relative circTIE1 expression
F
Relative miR-1286 expression
circTIE1-NC
circTIE1-KD1
circTIE1-KD2
LN229
T98G
G
miR-1286 3' UCCCGAGUAGAACCAGGACGU 5'
circTIE1 5' ... GGCGAGGAGACCAUCCUGCAG ... 3'
miR-1286 3' UCCCGAGUAGAACCAGGACGU 5'
circTIE1-wt 5' ... GGCGAGGAGACCAUCCUGCAG ... 3'
miR-1286 3' UCCCGAGUAGAACCUCGAGCU 5'
circTIE1-mt 5' ... GGCGAGGAGACCAUCCUGCAG ... 3'
H
LN229
miR-1286-NC
miR-1286-mimic
Relative luciferase activity
wt
mt
pGL3-circTIE1
I
T98G
miR-1286-NC
miR-1286-mimic
Relative luciferase activity
wt
mt
pGL3-circTIE1
J
LN229
miR-1286-NC
miR-1286-mimic
Relative enrichment of circTIE1
IgG
AgO
Input
K
LN229
miR-1286-NC
miR-1286-mimic
Relative enrichment of miR-1286
IgG
AgO
Input
L
T98G
miR-1286-NC
miR-1286-mimic
Relative enrichment of circTIE1
IgG
AgO
Input
M
T98G
miR-1286-NC
miR-1286-mimic
Relative enrichment of miR-1286
IgG
AgO
Input

Figure 3. CircTIE1 targets miR-1286 in glioma cells. (A) Identification of the miRNA that potentially regulated circTIE1 based on circIntercome and CSCD databases. (B-E) qPCR showed circTIE1 expression after miRNAs (miR-217, miR-555, miR-558, miR-595, miR-1205 and miR-1286) mimic (B, C) or inhibitor (D, E) treatment. (F) qPCR showed miR-1286 expression after circTIE1 knockdown in LN229 and T98G. (G) CircIntercome dataset showed the specific target site between circTIE1 and miR-1286. (H, I) Luciferase reporter assays showed the relative luciferase activity after miR-1286 treatment in LN229 and T98G. (J-M) The anti-Ago2 RNA immunoprecipitation (RIP) assay was performed in LN229 (J, K) and T98G (L, M) after the miR-1286 mimic treatment, followed by qPCR to detect the enrichment of circTIE1 and miR-1286. All data are shown as the mean ± SD (three independent experiments). **P < 0.05; **P < 0.01; ***P < 0.001.*

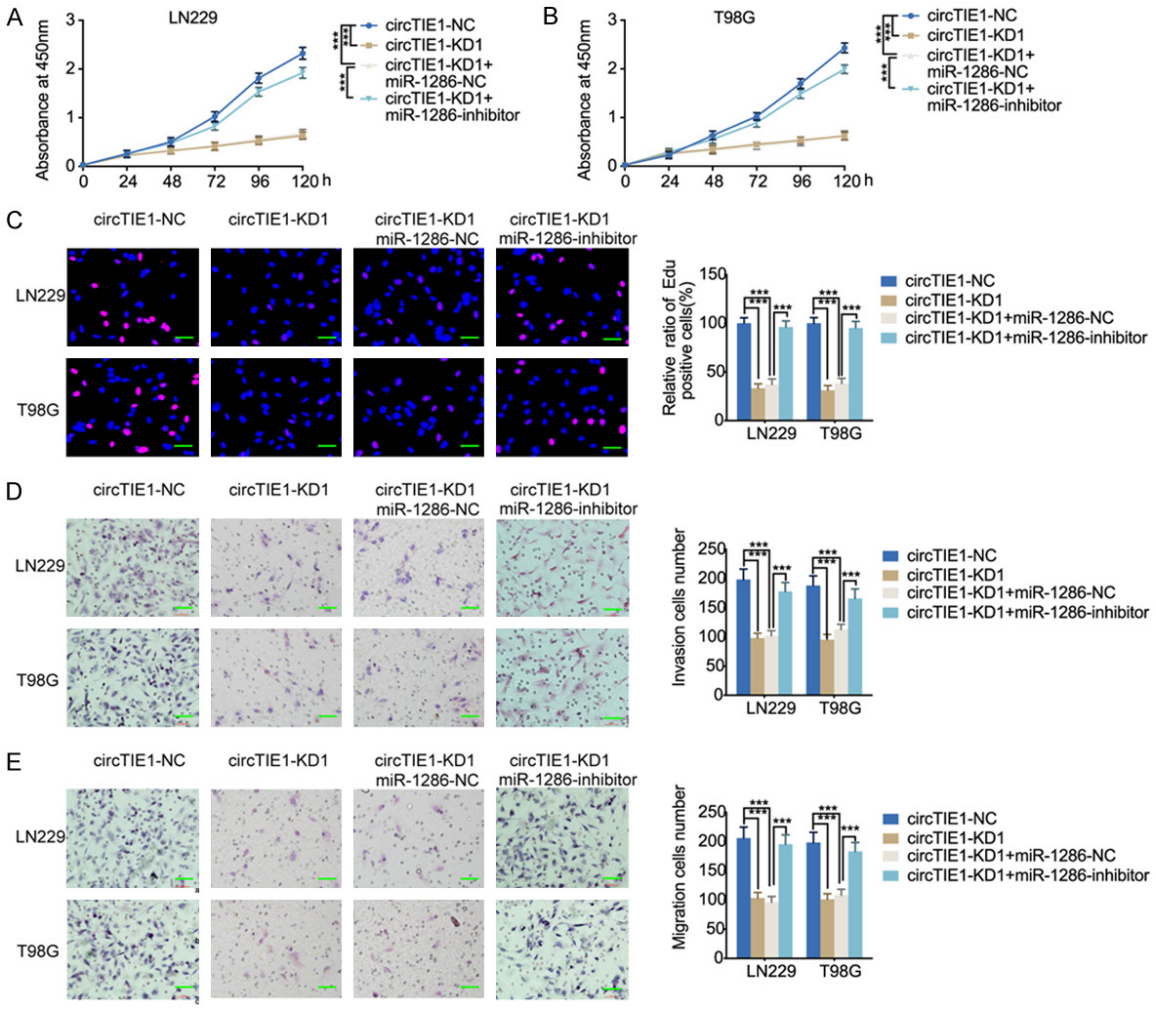

Figure 4. MiR-1286 inhibitor reverses the inhibiting effects of circTIE1 knockdown glioma cells. (A, B) MTS assays showed the cell viability of circTIE1 knockdown LN229 and T98G, followed by miR-1286 inhibitor treatment. (C) EDU assays showed the cell proliferation abilities of circTIE1 knockdown LN229 and T98G, followed with miR-1286 inhibitor treatment. Scale bar = 50 μm. (D, E) Transwell and migration assays showed the number of cell invasion (D) and migration (E) of circTIE1 knockdown LN229 and T98G, followed by miR-1286 inhibitor treatment. Scale bar = 50 μm. All data are shown as the mean ± SD (three independent experiments). **P < 0.05; **P < 0.01; ***P < 0.001.*

level did not vary obviously (**Figure 5B-E**). Therefore, TEAD1 is a downstream miR-1286 target gene. Furthermore, we obtained the specific target site between miR-1286 and the TEAD1 3'-UTR by means of the starBase database. We devised luciferase reporter assays accordingly (**Figure 5H**). The results indicated that the luciferase activities in the TEAD1 3'-UTR wild-type group were significantly increased after treatment with the miR-1286

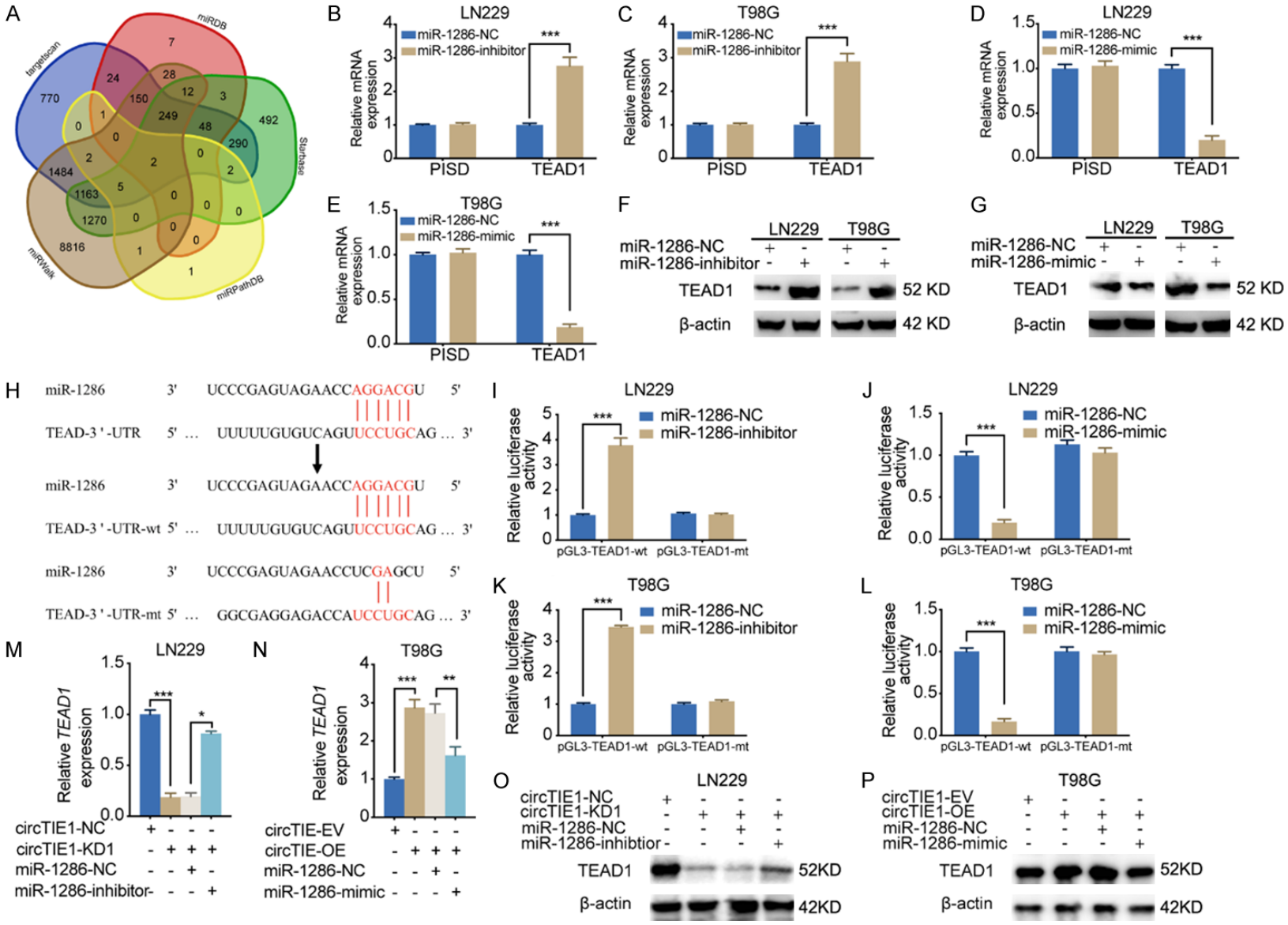

Figure 5. MiR-1286 directly targets TEAD1 in glioma cells. (A) Five datasets (Targetscan, miRDB, miRWalk, miRPathDB and Starbase) analysis was used to explore the potential target gene related to miR-1286. (B-E) qPCR assays were performed to detect the expression of PISD and TEAD1 after miR-1286 mimic (B, C) or inhibi-

tor (D, E) treatment in LN229 and T98G. (F, G) Western blotting showed the expression of TEAD1 after miR-1286 inhibitor (F) or mimic (G) treatment in LN229 and T98G. (H) Schematic diagram of the putative miR-1286 binding site in the 3'-UTR of TEAD1. (I-L) Luciferase assays showed the relative luciferase activities changes after miR-1286 mimic (I, K) or inhibitor (J, L) treatment in LN229 and T98G. (M, O) qPCR (M) and western blotting (O) showed the TEAD1 expression of circTIE1 knockdown LN229, followed by miR-1286 inhibitor treatment. (N, P) qPCR (N) and western blotting (P) showed the TEAD1 expression of circTIE1 overexpression T98G, followed by miR-1286 mimic treatment. All data are shown as the mean ± SD (three independent experiments). **P < 0.05; **P < 0.01; ***P < 0.001.*

inhibitor, while the luciferase activities were significantly decreased after treatment with the miR-1286 mimic (**Figure 5I-L**). Furthermore, to explore whether circTIE1 can competitively regulate the expression level of TEAD1 through miR-1286, we conducted qPCR and western blotting assays. We discovered that the TEAD1 expression level was obviously decreased after knockdown of circTIE1, while its expression was significantly restored after treatment with the miR-1286 inhibitor (**Figure 5M-P**), which confirmed that circTIE1 could upregulate the expression of TEAD1 by competitively antagonizing miR-1286 in glioma cells.

TEAD1 overexpression reverses the effects of circTIE1 knockdown on glioma cell proliferation and invasion

To confirm that circTIE1 promotes the malignant progression of glioma cells through TEAD1, we conducted rescue experiments by overexpressing TEAD1 in circTIE1-silenced glioma cell lines. EdU and MTS assays confirmed that cellular viability and proliferation abilities decreased significantly after circTIE1 knockdown, while cell viability and proliferation abilities recovered significantly after TEAD1 overexpression (**Figure 6A-C**). Transwell and migration assays also found that the quantity of cellular invasion and migration decreased significantly after circTIE1 knockdown, while the quantity of cellular aggression and migration recovered effectively after TEAD1 overexpression (**Figure 6D**, **6E**). The results above verify that circTIE1 facilitates glioma cellular aggression and proliferation through TEAD1.

TEAD1 overexpression reverses the effects of miR-1286 on glioma cell proliferation and invasion

To further demonstrate that miR-1286 inhibits the proliferation and invasion of glioma cells via TEAD1, we performed rescue experiments by overexpressing TEAD1 in glioma cell lines treated with miR-1286 mimics. EdU and MTS assays showed that glioma cell viability and proliferation abilities decreased after miR-1286 mimic treatment, while they were all increased after TEAD1 overexpression (**Figure 7A-C**). Transwell and migration assays also found that miR-1286 mimic treatment decreased the number of invading and migrating glioma cells, while they were all increased after TEAD1 overexpression (**Figure 7D**, **7E**). Therefore, the above results verify that miR-1286 inhibits glioma cellular aggression and proliferation by downregulating TEAD1.

Role of circTIE1 knockdown in the tumorigenicity of glioma cells

Although the above in vitro assays confirmed that circTIE1 can promote the aggression and proliferation of glioma cells, to verify the biological functions of circTIE1 in glioma, we carried out an intracranial tumorigenesis assay in nude mice. LN229 glioma cells in the circTIE1 control group or knockdown group were injected into the brain. After circTIE1 knockdown, the intracranial tumor volume of mice was significantly reduced (**Figure 8A**, **8B**), and the survival time was significantly prolonged (**Figure 8C**). We further used qPCR to detect tumor tissue samples and found that after knockdown of circTIE1, TEAD1 and circTIE1 expression levels were evidently decreased. Conversely, miR-1286 expression levels were apparently increased (**Figure 8D-F**). Furthermore, we used immunohistochemistry to detect that after circTIE1 silencing, the expression level of the proliferation-related gene Ki-67 was significantly reduced. Additionally, the TEAD1 expression level was also evidently decreased (**Figure 8G-I**). The above results in nude mice confirmed that circTIE1 actually plays a role in promoting glioma tumorigenesis. The possible function of the circTIE1/miR-1286/TEAD1 axis in glioma is shown in the model diagram (**Figure 8J**).

Discussion

Glioma is a kind of neuroepithelial tumor that accounts for 40%~60% of all main nucleus nervous system neoplasms as well as 81% of

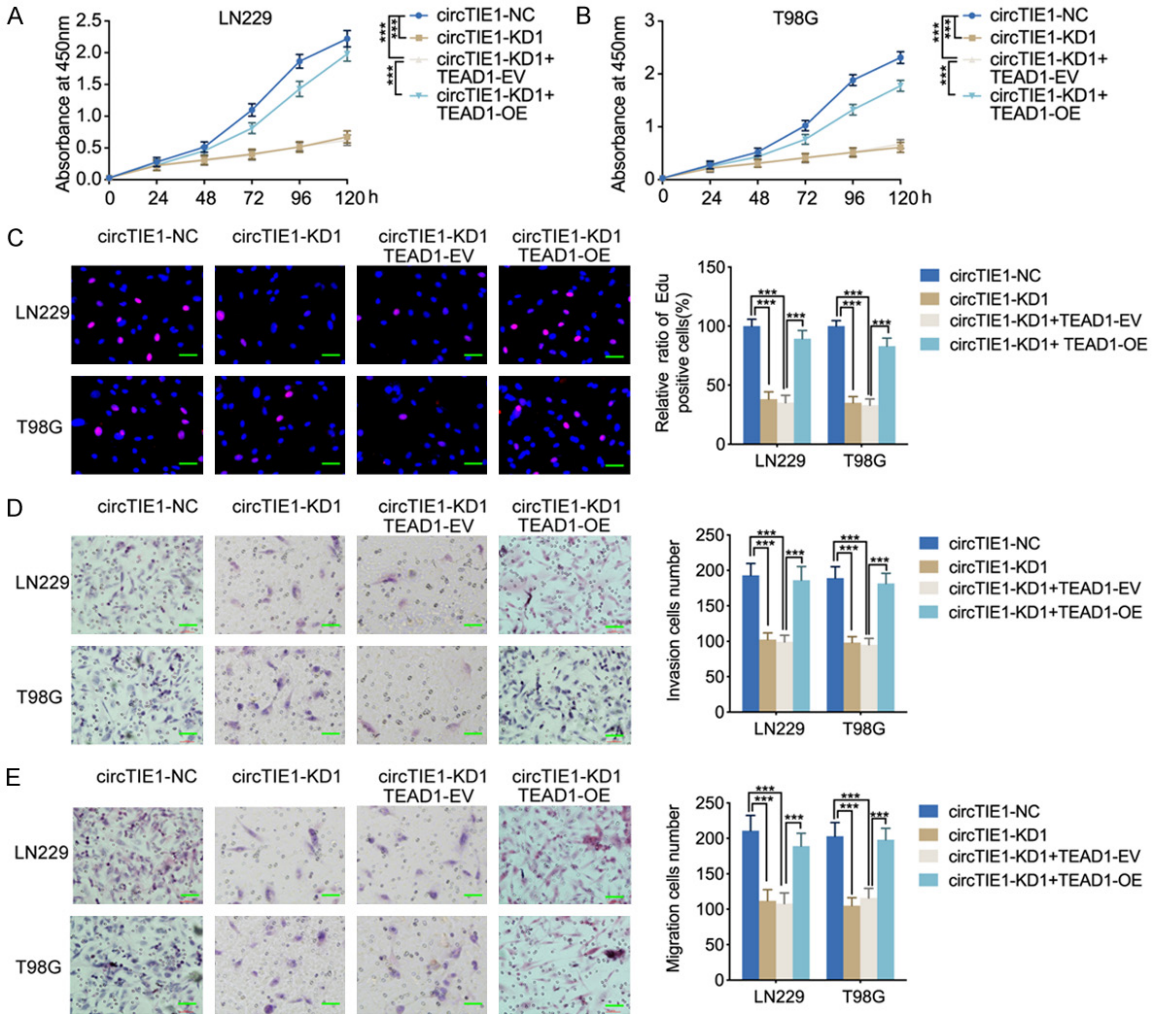

Figure 6. MiR-1286 inhibitor reverses the inhibiting effects of circTIE1 knockdown glioma cells. (A, B) MTS assays showed the cell viability of circTIE1 knockdown LN229 and T98G, followed by TEAD1 overexpression. (C) EDU assays showed the cell proliferation abilities of circTIE1 knockdown LN229 and T98G, followed with TEAD1 overexpression. Scale bar = 50 μm. (D, E) Transwell and migration assays showed the number of cell invasion (D) and migration (E) of circTIE1 knockdown LN229 and T98G, followed by TEAD1 overexpression. Scale bar = 50 μm. All data are shown as the mean ± SD (three independent experiments). **P < 0.05; **P < 0.01; ***P < 0.001.*

malignant central nervous system tumors. It is the most common main intracranial malignant neoplasm [21]. CircRNAs are widespread in eukaryotic cells and are formed by the covalent connection between downstream 5' splice donor sites as well as upstream 3' splice acceptor sites when lacking a 5' terminal cap structure as well as a 3' poly(A) tail [22]. CircRNAs are not readily decreased by means of RNA exonucleases (such as RNase R) and are steadier in comparison to linear RNAs. The circRNA formation mechanism includes RBP-driven cyclization, intron pairing-driven cyclization, and other cyclization mechanisms [22]. Many studies have shown that circRNAs play an excessively pivotal role in carcinoma. They can be utilized as possible carcinoma biomarkers and treatment targets.

In glioma, many new circRNAs with essential functions are found every year. However, compared with the large number of circRNAs and the complexity of the mechanism of glioma progression, there are still numerous circRNAs with unclear functions to be researched deeply. For our study, we performed circRNA sequencing and found that circTIE1 was one of the most significantly upregulated circRNAs in glioma, followed by clinical specimen validation. CircTIE1 expression was adjusted with increas-

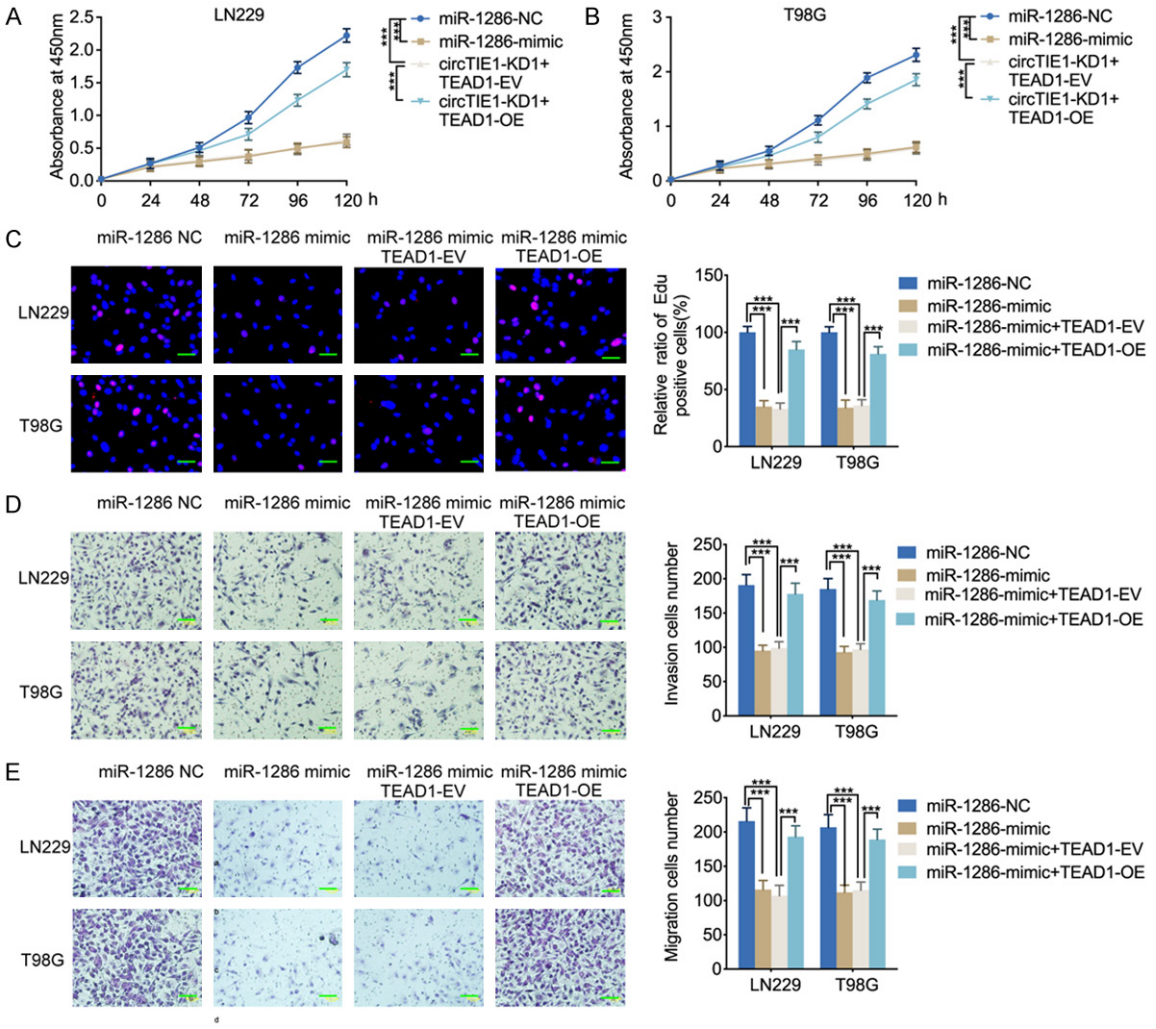

Figure 7. TEAD1 overexpression reverses the effects of miR-1286 on glioma cell proliferation and invasion. (A, B) MTS assays showed the cell viability of miR-1286 mimic treatment in LN229 and T98G, followed by TEAD1 overexpression. (C) EDU assays showed the cell proliferation abilities of miR-1286 mimic treatment in LN229 and T98G, followed with TEAD1 overexpression. Scale bar = 50 μm. (D, E) Transwell and migration assays showed the number of cell invasion (D) and migration (E) of miR-1286 mimic treatment LN229 and T98G, followed by TEAD1 overexpression. Scale bar = 50 μm. All data are shown as the mean ± SD (three independent experiments). **P < 0.05; **P < 0.01; ***P < 0.001.*

ing WHO grade, especially in grade IV. In addition, in vitro and in vivo experiments confirmed that circTIE1 plays a highly important role in promoting glioma cell viability, proliferation, invasion and migration.

CircRNAs participate in the organism's biological function and the progression of malignant tumors, mainly including the following mechanisms: miRNA molecular sponges, protein scaffolds or coding proteins. For example, circ_0000189 promotes glioma cell malignancy by adjusting the mir-192-5p-zeb2 axis [23]. CircLRFN5 is downregulated in glioma, binds to the PRRX2 protein, and promotes degradation by means of one ubiquitin-mediated proteasomal pathway [24]. CircHEATR5B is able to encode an emerging protein, HEATR5B-881aa, and blocks aerobic glycolysis in GBM [25]. MiRNA sponging is one of the most widely studied mechanisms in circRNA and other noncoding RNA studies. According to the prediction from the CSCD and circInteractome datasets, we found six miRNAs in intersections. After treatment of LN229 and T98G cells with either miRNA mimics or inhibitors, only miR-1286 was confirmed as the target miRNA that could bind to and regulate circTIE1.

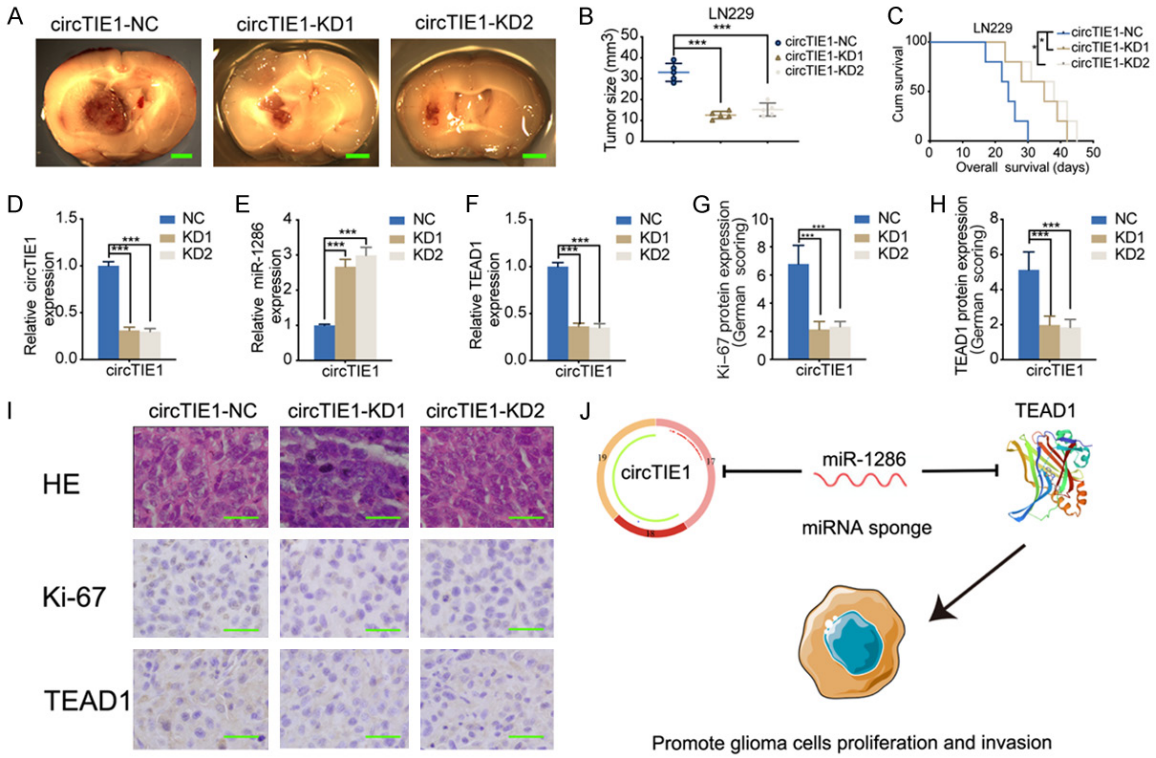

Figure 8. Role of circTIE1 knockdown in tumorigenicity of glioma cells. A, B: CircTIE1 knockdown inhibits tumor growth in vivo (n = 5, per group). Scale bar = 1 mm. C: Kaplan-Meier survival curve showed the survival time of circTIE1 knockdown LN229 inoculated mice (n = 5, per group). D-F: qPCR detect he expression levels of circTIE1, miR-1286 and TEAD1 in tumor tissue from circTIE1 knockdown LN229 inoculated mice. G, H: Quantitative analysis of IHC staining of ki-67 and TEAD1 according to the German immuno-histochemical scoring system. I: Representative immunohistochemical staining showed the changes in ki-67 and TEAD1 staining in tumor tissue from circTIE1 knockdown LN229 inoculated mice. Scale bar = 50 μm. J: Schematic diagram showed circTIE1 promotes the glioma cells viability, proliferation, migration and aggression via miR-1286 sponging TEAD1. All data are shown as the mean ± SD (three independent experiments). **P < 0.05; **P < 0.01; ***P < 0.001.*

MiR-1286 was discovered to play an exceedingly critical role in promoting cancer through the miRNA sponging mechanism in multiple malignant tumors. In gastric cancer, circCOL1A2 could promote cell invasion and migration via miR-1286 sponging to upregulate USP10 expression [26]. Circ_0051079 works as an oncogenic regulator inside osteosarcoma by competitively interacting with miR-1286 to upregulate the expression of MAFB [27]. However, several studies have also reported that miR-1286 might play an anti-neoplastic role via miRNA sponging. MiR-1286 is upregulated in ccRCC (clear cell renal cell carcinoma), and COL18A1-AS1 represses ccRCC progression by regulating KLF12 expression by competitively binding to miR-1286 [28]. Our study found that circTIE1 could target miR-1286 in LN229 and T98G glioma cells. MiR-1286 inhibitor treatment reversed the inhibitory effects of circTIE1 knockdown in glioma cells.

Our study further found that miR-1286 was able to bind to the TEAD1 3'-UTR and downregulate its expression. CircTIE1 knockdown downregulated the expression level of TEAD1, and its expression was significantly restored after treatment with a miR-1286 inhibitor. Functioning as one member of the TEA transcription element, TEAD1 is a critical oncogene in several cancers and an important targeted gene for miRNA sponging. It was reported that TEAD1 could promote hepatocellular carcinoma progression and exert a key role in the circCCT3/miR-1287-5p axis [29]. In non-small cell lung carcinoma, circTTBK2 facilitates malignancy by means of the miR-873-5p/DERL1/TEAD1 axis [30]. TEAD1 was also reported to participate in the malignant phenotype of glioma, and TEAD1 knockdown robustly diminished migration and altered migratory and EMT transcriptome signatures, both in vitro and in vivo [31]. TEAD1 could promote GBM proliferation,

migration and invasive characteristics, and YAP-TEAD1 association blockade is a viable treatment tactic for glioblastoma [32]. LINC-00473 could promote glioma advancement by means of miR-195-5p-mediated YAP1-TEAD1-Hippo signaling [33]. Our study found that TEAD1 overexpression reverses the effects of circTIE1 knockdown on glioma cellular aggression and proliferation.

In summary, this research proved that circTIE1 is a novel circRNA that is highly expressed in glioma cells and tissues. CircTIE1 promotes malignant biological activities of glioma by upregulating TEAD1 expression levels via miR-1286 sponging. Our research provides a greater understanding of circRNAs in the development and pathogenesis of glioma, is good for the diagnosis and treatment evaluation of glioma, and even provides a possible target for molecular targeted therapy of glioma.

Acknowledgements

This work was supported by the National Natural Science Foundation of China (grant number 81902531).

Written informed consent was obtained from all enrolled patients.

Disclosure of conflict of interest

None.

Abbreviations

NcRNAs, non-coding RNAs; circRNA, circular RNA; miRNAs, microRNAs; ceRNAs, competing endogenous RNAs; NBT, normal brain tissues; NHA, normal human astrocytes; H&E stain, hematoxylin and eosin stain; IHC, Immunohistochemistry; qRT-PCR/qPCR, Real-Time Quantitative Reverse Transcription polymerase chain reaction; RISC, RNA-induced silencing complex; ccRCC, clear cell renal cell carcinoma.

Address correspondence to: Xinrui Du, Department of Neurosurgery, Zibo Central Hospital, Zibo 255036, Shandong, China. E-mail: dxr1614@163.com

References

[1] De Silva MI, Stringer BW and Bardy C. Neuronal and tumourigenic boundaries of glioblastoma plasticity. Trends Cancer 2022; 9: 223-236.

[2] Gisina A, Kholodenko I, Kim Y, Abakumov M, Lupatov A and Yarygin K. Glioma stem cells: novel data obtained by single-cell sequencing. Int J Mol Sci 2022; 23: 14224.

[3] Szklener K, Mazurek M, Wieteska M, Wacławska M, Bilski M and Mańdziuk S. New directions in the therapy of glioblastoma. Cancers (Basel) 2022; 14: 5377.

[4] Bunse L, Bunse T, Krämer C, Chih YC and Platten M. Clinical and translational advances in glioma immunotherapy. Neurotherapeutics 2022; 19: 1799-1817.

[5] Bou Zerdan M, Atoui A, Hijazi A, Basbous L, Abou Zeidane R, Alame SM and Assi HI. Latest updates on cellular and molecular biomarkers of gliomas. Front Oncol 2022; 12: 1030366.

[6] Pan Z, Zhao R, Li B, Qi Y, Qiu W, Guo Q, Zhang S, Zhao S, Xu H, Li M, Gao Z, Fan Y, Xu J, Wang H, Wang S, Qiu J, Wang Q, Guo X, Deng L, Zhang P, Xue H and Li G. EWSR1-induced circNEIL3 promotes glioma progression and exosome-mediated macrophage immunosuppressive polarization via stabilizing IGF2BP3. Mol Cancer 2022; 21: 16.

[7] Peng D, Luo L, Zhang X, Wei C, Zhang Z and Han L. CircRNA: an emerging star in the progression of glioma. Biomed Pharmacother 2022; 151: 113150.

[8] Ahmed SP, Castresana JS and Shahi MH. Role of circular RNA in brain tumor development. Cells 2022; 11: 2130.

[9] Luo K, Liu A, Wu H, Liu Q, Dai J, Liu Y and Wang Z. CircKIF4A promotes glioma growth and temozolomide resistance by accelerating glycolysis. Cell Death Dis 2022; 13: 740.

[10] Liu L, Zhang P, Dong X, Li H, Li S, Cheng S, Yuan J, Yang X, Qian Z and Dong J. Circ_0001367 inhibits glioma proliferation, migration and invasion by sponging miR-431 and thus regulating NRXN3. Cell Death Dis 2021; 12: 536.

[11] Xu S, Luo C, Chen D, Tang L, Chen L and Liu Z. Whole transcriptome and proteome analyses identify potential targets and mechanisms underlying tumor treating fields against glioblastoma. Cell Death Dis 2022; 13: 721.

[12] Yin H, Wang H, Wang M, Yan Y, Dong Q, Li Q, Liu Y, Wang X, Guo T, Niu L, Zhang H, Wang B, Yao X, Yuan G and Pan Y. CircTCF25 serves as a sponge for miR-206 to support proliferation, migration, and invasion of glioma via the Jak2/p-Stat3/CypB axis. Mol Carcinog 2022; 61: 558-571.

[13] Pei Y, Zhang H, Lu K, Tang X, Li J, Zhang E, Zhang J, Huang Y, Yang Z, Lu Z, Li Y, Zhang H and Dong L. Circular RNA circRNA_0067934 promotes glioma development by modulating the microRNA miR-7/Wnt/β-catenin axis. Bioengineered 2022; 13: 5792-5802.

[14] Yuan F, Zhang S, Sun Q, Ye L, Xu Y, Xu Z, Deng G, Zhang S, Liu B and Chen Q. Hsa_circ_0072309 enhances autophagy and TMZ

sensitivity in glioblastoma. CNS Neurosci Ther 2022; 28: 897-912.
[15] Li C, Guan X, Jing H, Xiao X, Jin H, Xiong J, Ai S, Wang Y, Su T, Sun G, Fu T, Wang Y, Guo S and Liang P. Circular RNA circBFAR promotes glioblastoma progression by regulating a miR-548b/FoxM1 axis. FASEB J 2022; 36: e22183.
[16] Jiang Y, Wang Z, Ying C, Hu J, Zeng T and Gao L. FMR1/circCHAF1A/miR-211-5p/HOXC8 feedback loop regulates proliferation and tumorigenesis via MDM2-dependent p53 signaling in GSCs. Oncogene 2021; 40: 4094-4110.
[17] Huang T, Kim CK, Alvarez AA, Pangeni RP, Wan X, Song X, Shi T, Yang Y, Sastry N, Horbinski CM, Lu S, Stupp R, Kessler JA, Nishikawa R, Nakano I, Sulman EP, Lu X, James CD, Yin XM, Hu B and Cheng SY. MST4 phosphorylation of ATG4B regulates autophagic activity, tumorigenicity, and radioresistance in glioblastoma. Cancer Cell 2017; 32: 840-855.e8.
[18] Jiang Y, Zhou J, Hou D, Luo P, Gao H, Ma Y, Chen YS, Li L, Zou D, Zhang H, Zhang Y and Jing Z. Prosaposin is a biomarker of mesenchymal glioblastoma and regulates mesenchymal transition through the TGF-beta1/Smad signaling pathway. J Pathol 2019; 249: 26-38.
[19] Tan Z, Jiang Y, Liang L, Wu J, Cao L, Zhou X, Song Z, Ye Z, Zhao Z, Feng H, Dong Z, Lin S, Zhou Z, Wang Y, Li X and Guan F. Dysregulation and prometastatic function of glycosyltransferase C1GALT1 modulated by cHP1BP3/miR-1-3p axis in bladder cancer. J Exp Clin Cancer Res 2022; 41: 228.
[20] Wu D, Chen T, Zhao X, Huang D, Huang J, Huang Y, Huang Q, Liang Z, Chen C, Chen M, Li D, Wu B and Li L. HIF1α-SP1 interaction disrupts the circ-0001875/miR-31-5p/SP1 regulatory loop under a hypoxic microenvironment and promotes non-small cell lung cancer progression. J Exp Clin Cancer Res 2022; 41: 156.
[21] Wesseling P and Capper D. WHO 2016 classification of gliomas. Neuropathol Appl Neurobiol 2018; 44: 139-150.
[22] Wang D, Li R, Jiang J, Qian H and Xu W. Exosomal circRNAs: novel biomarkers and therapeutic targets for gastrointestinal tumors. Biomed Pharmacother 2022; 157: 114053.
[23] Yang J, Hou G, Chen H, Chen W and Ge J. Circ_0000189 promotes the malignancy of glioma cells via regulating miR-192-5p-ZEB2 axis. Oxid Med Cell Longev 2022; 2022: 2521951.
[24] Jiang Y, Zhao J, Li R, Liu Y, Zhou L, Wang C, Lv C, Gao L and Cui D. CircLRFN5 inhibits the progression of glioblastoma via PRRX2/GCH1 mediated ferroptosis. J Exp Clin Cancer Res 2022; 41: 307.
[25] Song J, Zheng J, Liu X, Dong W, Yang C, Wang D, Ruan X, Zhao Y, Liu L, Wang P, Zhang M and Liu Y. A novel protein encoded by ZCRB1-induced circHEATR5B suppresses aerobic glycolysis of GBM through phosphorylation of JMJD5. J Exp Clin Cancer Res 2022; 41: 171.
[26] Li H, Chai L, Ding Z and He H. CircCOL1A2 sponges miR-1286 to promote cell invasion and migration of gastric cancer by elevating expression of USP10 to downregulate RFC2 ubiquitination level. J Microbiol Biotechnol 2022; 32: 938-948.
[27] Huang Z, Chen P, Jia R and Liu Y. Circ_0051079 functions as an oncogenic regulator in osteosarcoma by leading to MAFB expression upregulation by competitively interacting with miR-1286. J Orthop Surg Res 2022; 17: 428.
[28] Liu Y, Wang J, Shou Y, Xu W, Huang Z, Xu J, Chen K, Liu J, Liu D, Liang H, Yang H and Zhang X. Restoring the epigenetically silenced lncRNA COL18A1-AS1 represses ccRCC progression by lipid browning via miR-1286/KLF12 axis. Cell Death Dis 2022; 13: 578.
[29] Lin W, Zhang T, Ding G, Hao L, Zhang B, Yu J, Pang Y, Geng F, Zhan L, Zhou M, Yan Q, Wang Y, Zheng C and Li H. Circular RNA circ-CCT3 promotes hepatocellular carcinoma progression by regulating the miR-1287-5p/TEAD1/PTCH1/LOX axis. Mol Med Rep 2021; 23: 375.
[30] Wei JY, Zhang Q, Yao Y, He HB, Sun CH, Dong TT, Meng GP and Zhang J. Circular RNA circTTBK2 facilitates non-small-cell lung cancer malignancy through the miR-873-5p/TEAD1/DERL1 axis. Epigenomics 2022; 14: 931-949.
[31] Tome-Garcia J, Erfani P, Nudelman G, Tsankov AM, Katsyv I, Tejero R, Bin Z, Walsh M, Friedel RH, Zaslavsky E and Tsankova NM. Analysis of chromatin accessibility uncovers TEAD1 as a regulator of migration in human glioblastoma. Nat Commun 2018; 9: 4020.
[32] Saunders JT, Holmes B, Benavides-Serrato A, Kumar S, Nishimura RN and Gera J. Targeting the YAP-TEAD interaction interface for therapeutic intervention in glioblastoma. J Neurooncol 2021; 152: 217-231.
[33] Wang X, Li XD, Fu Z, Zhou Y, Huang X and Jiang X. Long non-coding RNA LINC00473/miR-195-5p promotes glioma progression via YAP1-TEAD1-Hippo signaling. Int J Oncol 2020; 56: 508-521.